On the stability of artificial equilibrium points in the circular restricted three-body problem

Claudio Bombardelli · Jesus Peláez

Abstract The article analyses the stability properties of minimum-control artificial equilibrium points in the planar circular restricted three-body problem. It is seen that when the masses of the two primaries are of different orders of magnitude, minimum-control equilibrium is obtained when the spacecraft is almost coorbiting with the second primary as long as their mutual distance is not too small. In addition, stability is found when the distance from the second primary exceeds a minimum value which is a simple function of the mass ratio of the two primaries and their separation. Lyapunov stability under non-resonant conditions is demonstrated using Arnold's theorem. Among the most promising applications of the concept we find solar-sail-stabilized observatories coorbiting with the Earth, Mars, and Venus.

Keywords Three-body problem · Artficial equilibrium points · Stability · Solar sails

1 Introduction

The use of artificial equilibrium points (AEPs) have received considerable attention in the last decade as a means to stabilize a spacecraft in a region of space where equilibrium is not possible with gravitational forces alone but can be achieved by means of man-made propulsion devices providing continuous acceleration. Propellantless propulsion systems such as solar sails and electrodynamic tethers are ideal candidates for this concept as they open up the possibility of placing permanent or very long term outposts at different points of interest in space. These could serve the purpose of scientific observatories, communication stations or even habitable modules for astronauts in the far future.

The subject of artificial equilibrium points has been studied extensively in the literature. In 1990 Forward (1991) first proposed the deployment of a stationary satellite hovering above the Earth poles with solar radiation pressure balancing gravitational forces.

McInnes and McDonald in (1994) derived continuous surfaces of unstable AEPs in the circular restricted three-body problem (CRTBP) when a low-thrust control acceleration was added. Nevertheless, it was not until 2007 that Morimoto et al. (2007) realized that linear (i.e. marginal) stability could be found in a region of space far enough from the second primary. Morimoto also noticed that linearly stable equilibrium positions belonging to the orbital plane of the two primaries required the smallest amount of control acceleration, which for the case of the Earth–Sun system could be smaller than 5×10^{-5} m/s^2. Although the issue of nonlinear stability was discussed by the previous author only a numerical simulation was provided to show a "qualitatively stable" behaviour in three dimensions. In the same year, and unaware of the previous study, Pelaez and Scheeres (2007) found a linearly stable region while studying the dynamics of an electrodynamic tether located in the proximity of the inner Jupiter moons. Using a Hill formulation of the circular three-body problem they showed that a tethered system located in the orbital path of the moon at a distance greater than a given value enjoyed linear stability. The results obtained by Morimoto were confirmed by Baig and McInnes (2008) who proposed to control the AEPs with a hybrid solar sail and electric propulsion system.

In this article we analyze the stability of artificial equilibrium positions in the planar CRTBP focusing on the need to minimize the required control acceleration. First, we investigate the linear stability of the artificial equilibrium position with a series expansion of the system Hamiltonian which is later used to investigate non-linear (Lyapunov) stability. Next, we compute the locus of the points belonging to the plane of the two primaries for which equilibrium is obtained with minimum acceleration as a function of the distance between the spacecraft and the second primary. An approximate analytical solution is obtained with a straightforward perturbation technique in which the small parameter is the mass ratio μ of the two primaries. The solution is employed to compute the intersection between the minimum-control curve and the previously derived stability region. By exploiting the smallness of μ we derive simple and quite accurate analytical expressions to quantify the distance of the closest stable equilibrium point from the second primary and the magnitude of the required control acceleration. The location of resonance points in the stable region, for which stability cannot be granted on the base of a linear analysis, is also computed and simple analytical expressions are provided. Finally a survey of promising three-body "gravitational environments" in our solar system is performed highlighting the most favorable places to be considered for an application of the results obtained. Numerical simulations of the complete equations of motion are included in order to verify the validity of the proposed solution.

2 Equations of motion

Under the framework of the circular restricted three-body problem (CRTBP) we denote $M_1 = (1-\mu)M$ and $M_2 = \mu M$ to be the masses of the first and second primary, respectively. Here M is the total mass of the system and ℓ the distance between the primaries. The two primaries revolve around each other at angular velocity:

$$\omega = \sqrt{\frac{GM}{\ell^3}},$$

where G is the gravitational constant. We introduce a synodic coordinate system $(\boldsymbol{u}_x, \boldsymbol{u}_y, \boldsymbol{u}_z)$ with origin at the second primary and rotating with angular velocity $\boldsymbol{\omega} = \omega \boldsymbol{u}_z$ around an axis orthogonal to their orbital plane, with $\boldsymbol{u}_x$ along the line going from the first to the second primary. We then consider a spacecraft (third body) of mass m placed in the xy

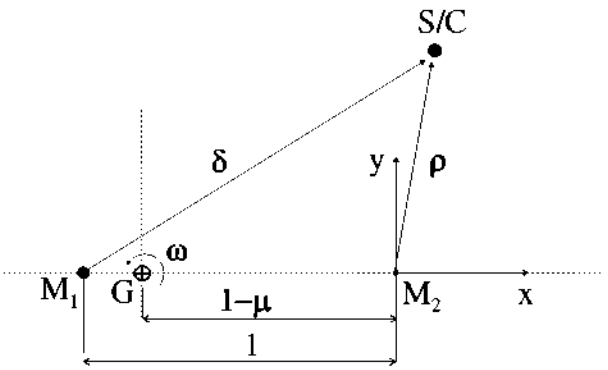

Fig. 1 Schematic of synodic plane and spacecraft position

plane at a distance ρ from the second primary and δ from the first, and undergoing a constant acceleration to maintain it in the neighborhood of its initial position (x_0, y_0) (Fig. 1).

From now on we will write all physical quantities in dimensionless coordinates taking as ℓ the unit of distance and as $1/\omega$ the unit of time. The spacecraft position vector measured from the center of mass of the two primaries can then be written as:

$$\mathbf{r} = (\mathbf{1} - \mu + \mathbf{x}, \mathbf{y})^{\mathbf{T}},$$

while the spacecraft distance from the first and second primary are, respectively:

$$\delta = \sqrt{x^2 + y^2 + 2x + 1}, \tag{1}$$

$$\rho = \sqrt{x^2 + y^2}. \tag{2}$$

Equations (1, 2) can be inverted for later use providing:

$$x = \frac{\delta^2 - \rho^2 - 1}{2}, \tag{3}$$

$$y = \pm\frac{1}{2}\sqrt{4\rho^2 - (\delta^2 - \rho^2 - 1)^2}, \tag{4}$$

with the contraint:

$$|1 - \rho| < \delta < 1 + \rho. \tag{5}$$

The inertial kinetic energy per unit mass is given by:

$$T = \frac{1}{2}\|\dot{\boldsymbol{r}} + \boldsymbol{\omega} \times \boldsymbol{r}\|^2 = \frac{1}{2}(\dot{x}^2 + \dot{y}^2) + \dot{y}(x + 1 - \mu) - \dot{x}y + \frac{1}{2}(x^2 + y^2) + x(1 - \mu). \tag{6}$$

The total potential due to the gravitational and the constant control acceleration is:

$$V = V_g + V_a = -\frac{1 - \mu}{\delta} - \frac{\mu}{\rho} - a_x x - a_y y. \tag{7}$$

where a_x, a_y are the x and y components of the control acceleration (Fig. 1).

The equations of motion can finally be derived through Lagrange equations and yield:

$$\ddot{x} - 2\dot{y} = 1 - \mu + x - (1-\mu)\frac{1+x}{\delta^3} - \mu\frac{x}{\rho^3} + a_x,$$

$$\ddot{y} + 2\dot{x} = y - (1-\mu)\frac{y}{\delta^3} - \mu\frac{y}{\rho^3} + a_y.$$

The control acceleration for maintaining a desired equilibrium position (x_0, y_0) is hence:

$$a_x = (1-\mu)\frac{1+x_0}{\delta_0^3} + \mu\frac{x_0}{\rho_0^3} - x_0 + \mu - 1, \tag{8}$$

$$a_y = (1-\mu)\frac{y_0}{\delta_0^3} + \mu\frac{y_0}{\rho_0^3} - y_0, \tag{9}$$

where δ_0, ρ_0 are the radial distances of the equilibrium point from the first and second primary, respectively.

3 Linear stability conditions

In this section we will study the linear stability of the system using a Hamiltonian approach which will be later extended to the investigation of non-linear stability.

From the kinetic and potential energy we obtain the Lagrangian function:

$$L = T - V,$$

which provides the canonical Hamiltonian variables:

$$p_x = \frac{\partial L}{\partial x} = \dot{x} - y,$$

$$p_y = \frac{\partial L}{\partial y} = \dot{y} + x + 1 - \mu,$$

so that the Hamiltonian can be derived as:

$$H = p_x\dot{x} + p_y\dot{y} - L,$$

yielding:

$$H = \frac{1}{2}(p_x^2 + p_y^2) + p_x y - p_y(x + 1 - \mu) - \frac{1-\mu}{\delta} - \frac{\mu}{\rho} - a_x x - a_y y.$$

In order to study the linear (local) equilibrium it is convenient to write the Hamiltonian with respect to o reference system with origin at the equilibrium point. This can be done by the following change of variables:

$$\xi = x - x_0,$$

$$\eta = y - y_0,$$

$$p_\xi = p_x - p_{x0} = p_x + y_0,$$

$$p_\eta = p_y - p_{y0} = p_y - x_0 - 1 + \mu,$$

which after eliminating constant terms yields the Hamiltonian:

$$H = \frac{1}{2}(p_\xi^2 + p_\eta^2) + p_\xi\eta - p_\eta\xi + \xi(\mu - 1 - x_0) - \eta y_0 - \frac{1-\mu}{\delta} - \frac{\mu}{\rho} - a_x\xi - a_y\eta, \tag{10}$$

where:

$$\delta = \sqrt{(1+\xi+x_0)^2+(\eta+y_0)^2},$$
$$\rho = \sqrt{(\xi+x_0)^2+(\eta+y_0)^2}.$$

Because the origin is an equilibrium point H can be expanded in series in which the linear term disappears:

$$H = H_2 + \sum_{k>2} H_k, \tag{11}$$

where:

$$H_2 = \frac{1}{2}(p_\xi^2 + p_\eta^2) + \eta p_\xi - \xi p_\eta + a\xi^2 + b\xi\eta + c\eta^2, \tag{12}$$

and where a, b, c are function of the equilibrium point location and can be conveniently written in bipolar coordinates:

$$\begin{aligned}
a &= -\frac{\mu}{8\rho^5}\left(3\delta^4 - 6\delta^2\rho^2 - 6\delta^2 + 3\rho^4 + 2\rho^2 + 3\right) \\
&\quad -\frac{1-\mu}{8\delta^5}\left(3\rho^4 - 6\rho^2\delta^2 - 6\rho^2 + 3\delta^4 + 2\delta^2 + 3\right), \\
b &= -\frac{3\sqrt{2\rho^2(\delta^2+1) - (\delta^2-1)^2 - \rho^4}}{4\rho^5\delta^5}\Big[\rho^5\delta^2 - \rho^7, \\
&\quad + \rho^5 + \mu(-\delta^5 + \delta^7 - \delta^5\rho^2 - \rho^5 - \rho^5\delta^2 + \rho^7)\Big] \\
c &= \frac{\mu}{8\rho^5}\left(3\delta^4 - 6\delta^2\rho^2 - 6\delta^2 + 3\rho^4 + 2\rho^2 + 3\right) \\
&\quad +\frac{1-\mu}{8\delta^5}\left(3\rho^4 - 6\rho^2\delta^2 - 6\rho^2 + 3\delta^4 - 2\delta^2 + 3\right),
\end{aligned}$$

The linearized equations of motion are finally:

$$\begin{aligned}
\dot{p}_\xi &= -\frac{\partial H_2}{\partial \xi} = p_\eta - 2a\xi - b\eta, \\
\dot{p}_\eta &= -\frac{\partial H_2}{\partial \eta} = -p_\xi - 2c\eta - b\xi, \\
\dot{\xi} &= \frac{\partial H_2}{\partial p_\xi} = p_\xi + \eta, \\
\dot{\eta} &= \frac{\partial H_2}{\partial p_\eta} = p_\eta - \xi,
\end{aligned}$$

with the corresponding Jacobian matrix:

$$A = \begin{bmatrix} 0 & 1 & -2a & -b \\ -1 & 0 & -b & -2c \\ 1 & 0 & 0 & 1 \\ 0 & 1 & -1 & 0 \end{bmatrix}$$

and the characteristic polynomial:

$$P(\lambda) = \lambda^4 + 2f\lambda^2 + g \tag{13}$$

where f, g can be written as:

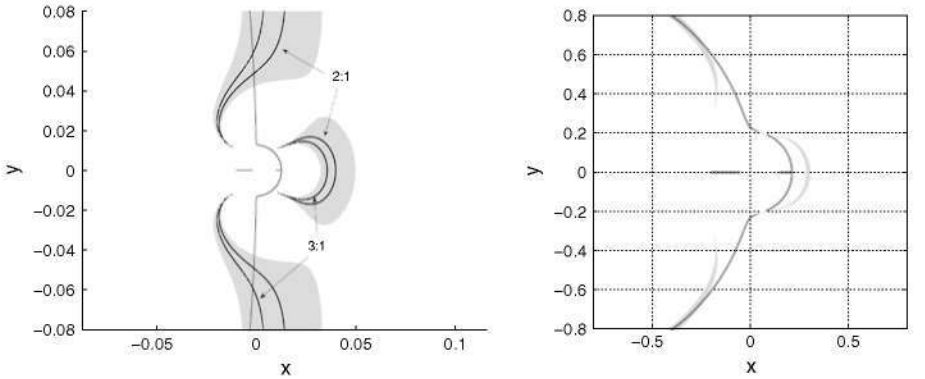

Fig. 2 Stability boundary for the Sun–Earth system (*left*) ($\mu = 3.0 \times 10^{-6}$) and for the Earth–Moon system (*right*) ($\mu = 1.2 \times 10^{-2}$). The *light grey* area delimits the stable zone while the *dark grey solid line* represents the minimum-control equilibrium points computed by numerically solving Eq. (27). The *dark lines* on the *left* figure represents equilibrium points with (2:1) and (3:1) resonance. Distances are measured with respect to the second primary in units of separation between the two primaries (ℓ)

$$f = a + c + 1 = \frac{2\delta^3 - 1}{2\delta^3} + \mu \frac{\rho^3 - \delta^3}{2\rho^3\delta^3}, \tag{14}$$

$$\begin{aligned} g = -b^2 + 2a(c-1) - 2c + 1 = {} & \frac{\delta^6 - 2 + \delta^3}{\delta^6} + \frac{\mu}{4\rho^5\delta^6}\left(-4\rho^5\delta^3\right. \\ & \left. +16\rho^5 + 4\rho^2\delta^6 + 18\rho^2\delta + 18\delta^3 - 9\delta^5 + 2\rho^2\delta^3 - 9\delta\rho^4 - 9\delta\right) \\ & - \frac{\mu^2}{4\rho^6\delta^6}\left(-9\rho\delta^5 + 18\rho\delta^3 - 9\rho^5\delta + 18\rho^3\delta + 8\delta^6 - 9\rho\delta + 8\rho^6 + 2\delta^3\rho^3\right), \end{aligned} \tag{15}$$

In order for the characteristic polynomial (13) to have pure imaginary roots the following conditions have to be satisfied:

$$\begin{aligned} &a) \quad f^2 - g > 0, \\ &b) \quad f > 0, \\ &c) \quad g > 0. \end{aligned} \tag{16}$$

The three conditions delimit a stable region in the orbital plane of the two primaries which is plotted in Figs. 2 and 3 for three different values of the contant μ. The stability region for the Earth-Sun system was already obtained by Morimoto et al. (2007) although an explicit analytical representation of the Curves was not provided.

We point out to the reader that, as an alternative to our Hamiltonian approach, it is possible and straightforward to study the system linear stability by just calculating the variational equations of the Cartesian equations of motion.

4 Nonlinear stability

As it is known, when a linearized system has all its eigenvalues in the left-half complex plane but at least one on the $j\omega$ axis (i.e. the system is marginally stable) one cannot infer stability from the linear part alone, as higher order terms can drive the system towards instability. This

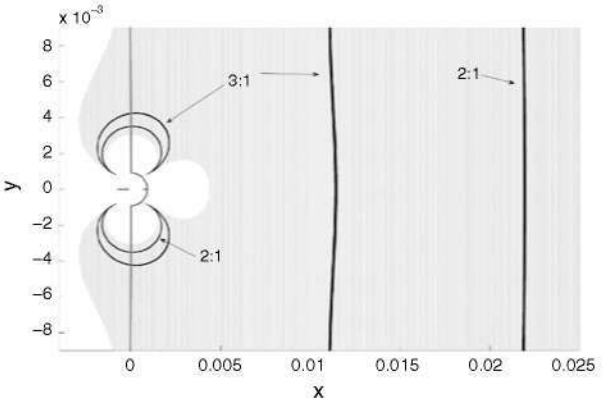

Fig. 3 Stability boundary for the Jupiter–Amalthea system ($\mu = 1.1 \times 10^{-9}$). The *light grey* area delimits the stable zone while the *dark grey solid line* represents the minimum-control equilibrium points computed by numerically solving Eq. (27). The *dark lines* represents equilibrium points with (2:1) and (3:1) resonance. Distances are measured with respect to the second primary in units of separation between the two primaries (ℓ)

is also the case of the triangular Lagrangian points in the CRTBP whose Lyapunov stability, for the two dimensional case, was first demonstrated by Leontovitch in (1962) by investigating higher order terms of the system Hamiltonian and with the aid of Arnold's stability theorem. Leontovitch showed that the system was stable for all values of the the mass ratio satisfying $0 < \mu < (9 - \sqrt{69})/18 \simeq 0.0385, \ldots$, with the exclusion of a set of values of measure zero for which no conclusion about stability could be made. Later on, Deprit and Deprit-Bartholome (1967) proved that the zero-measure set consisted of only three points: $\mu_1 = (45 - \sqrt{1833})/90 \simeq 0.0243$, $\mu_2 = (15 - \sqrt{213})/30 \simeq 0.0135$, $\mu_3 = 0.0109$ the first two corresponding to 2:1 and 3:1 resonances between the two normal frequencies of oscillations around the Lagrangian point, while the third having no straightforward physical meaning. Markeev, in (1972), proved the instability of the two resonance values while stability was found for the third value.

Arnold's stability theorem can be applied to our case to guarantee Lyapunov stability along the whole linearly stable domain with the exception of a set of points with zero measure.

From the previous linearization we can derive the two oscillation frequencies around the AEP as:

$$i\omega_{1,2} = \sqrt{-f \pm \sqrt{f^2 - g}},$$

$$\omega_{1,2} = \sqrt{\frac{2\rho^3\delta^3 - \rho^3 + \mu\rho^3 - \mu\delta^3 \pm \sqrt{K}}{2\rho^3\delta^3}}, \tag{17}$$

where

$$K = -8\rho^6\delta^3 + 9\rho^6 - \rho\left(18\rho^5 - 8\rho^5\delta^3 + 8\delta^6\rho^2 - 9\delta - 9\delta^5 + 18\delta^3 + 18\delta\rho^2 - 9\delta\rho^4\right)\mu$$
$$+9\left(2\rho^3\delta + 2\rho\delta^3 - \rho\delta^5 - \delta\rho - \rho^5\delta + \rho^6 + \delta^6\right)\mu^2. \tag{18}$$

According to Arnold's theorem the marginally stable equilibrium point $(p_\xi, p_\eta, \xi, \eta) = (0, 0, 0, 0)$ is Lyapunov stable if two conditions are verified. The first, known as the *nonresonance condition* imposes that:

$$k_1\omega_1 + k_2\omega_2 \neq 0, \tag{19}$$

for all pairs of rational integers such that:

$$|k_1| + |k_1| \leq 4.$$

The second, known as the *reversibility condition* reads:

$$A\omega_1^2 + B\omega_1\omega_2 + C\omega_2^2 \neq 0, \tag{20}$$

where A, B, C are the coefficient of the fourth order part of the normalized Hamiltonian [see ref. Deprit and Deprit-Bartholome (1967)]:

$$\bar{H}_4 = \frac{1}{2}(AI_1^2 + BI_1I_2 + CI_2^2)$$

with:

$$I_1 = \frac{\bar{p}_\xi^2 + \bar{\xi}^2}{2}; \quad I_2 = \frac{\bar{p}_\eta^2 + \bar{\eta}^2}{2},$$

and where $(\bar{p}_\xi, \bar{p}_\eta, \bar{\xi}, \bar{\eta})$ are the new Hamiltonian variables after the normalization.

It can be readily verified that condition (19) leads to the exclusion of the two resonance cases:

$$\omega_1 = 2\omega_2, \tag{21}$$

$$\omega_1 = 3\omega_2, \tag{22}$$

Equations (21–22) represent two curves in the orbital plane which can be obtained in bipolar coordinates using Eqs. (17, 18). After some algebra one obtains the 2:1 resonance curve as:

$$\begin{aligned}
&(-36\rho^6 - 164\mu\rho^3 + 216\nu^2)\delta^6 + 225(-\mu^2\rho + \mu\rho)\delta^5 \\
&+ (450\mu\rho + 18\mu^2\rho^3 - 18\mu\rho^3 + 164\mu\rho^6 - 164\rho^6 + 450\mu^2\rho)\delta^3 \\
&+ 225(\mu\rho^5 - \mu^2\rho^5 + 2\mu^2\rho^3 - \mu^2\rho + \mu\rho - 2\mu\rho^3)\delta \\
&+ 216(-2\mu\rho^6 + \mu^2\rho^6 + \rho^6) = 0,
\end{aligned} \tag{23}$$

while the 3:1 resonauce curve yields:

$$\begin{aligned}
&(-64\rho^6 - 136\mu\rho^3 + 209\mu^2)\delta^6 + 225(-\mu^2\rho + \mu\rho)\delta^5 \\
&+(-450\mu\rho + 32\mu^2\rho^3 - 32\mu\rho^3 + 136\mu\rho^6 - 136\rho^6 + 450\mu^2\rho)\delta^3 \\
&+ 225(\mu\rho^5 - \mu^2\rho^5 + 2\mu^2\rho^3 - \mu^2\rho + \mu\rho - 2\mu\rho^3)\delta \\
&+ 209(-2\mu\rho^6 + \mu^2\rho^6 + \rho^6) = 0.
\end{aligned} \tag{24}$$

The curves cut through the stability domain as plotted in Figs. 2 and 3. Along those arcs Arnold's theorem cannot assure Lyapunov stability although the similarity with the case of the L_4, L_5 Lagrangian points in the CRTBP would suggest the arcs are unstable. A stability analysis along the three resonaut arcs is beyoud the scope of the present article.

Similarily, condition (20) represents auother curve iu the orbital plane which will iutersect the stable region. Along the resulting arcs stability or instability needs to be inferred by normalization of higher order terms in the Hamiltonian series expansion. Given the complexity of the normalization procedure, the derivation of curve (20) will not be dealt with in the present article.

As far as the three-dimensional problem is concerned, "effective stability" can be assured given the analogy of the present problem with the triangular Lagrangian poiuts iu the CRTBP. The latter has been shown to be stable iu three dimeusious (although not in the sense of Lyapunov) by Markeev (1972). Celletti and Giorgilli (1991) also dealt with the problem of finding effective stability for the system (i.e. according to Nekhoroshev theory) and the interested reader can check the reference mentioned above.

5 Minimum control artificial equilibrium points

After having demonstrated the existence of a stable region in the planar perturbed CRTBP the next step is to identify stable points inside this region for which the required control acceleration is as small as possible. In this regard, our proposed approach is to fix an equilibrium distance ρ_0 from the second primary and to search for the spacecraft position that provides minimum control acceleration. This corresponds to minimize the objective function:

$$J = a_x^2 + a_y^2, \tag{25}$$

for a fixed value of ρ_0. Using Eqs. (3, 4) we can eliminate the variables x, y from Eqs. (8–25) and express J in bipolar coordinates. Omitting the subscript '0' from δ, ρ in order to simplify the notation we obtain:

$$J(\rho,\delta) = \frac{\mu(\rho^3-1)(\rho-1)(\mu+\rho^2+\rho)}{\rho^4} - \frac{1-\mu}{\rho^3\delta^4} \times \left[(\mu-\rho^3)\delta^6 - (\mu-2\rho^3+\mu\rho^3)\delta^3 + \mu(\rho^3-1)(\rho^2-1)\delta - (1-\mu)\rho^3\right],$$

subject to contraint (5).

Given the complex structure of the function J we decided to first study the minimization problem numerically using a grid-sampling approach. Figure 4, dealing with the Earth–Moon and Sun–Earth systems respectively, represent the locus of the equilibrium points that, for a fixed value of the distance from the second primary, are characterized by minimum control acceleration. Taking for instance the Earth–Moon system as an example (Fig. 4) we see that when ρ is large compared with the distances ρ_{L1}, ρ_{L2} between the second primary and the two Lagrangian points minimum acceleration is obtained when the spacecraft is almost coorbiting with the second primary. As ρ decreases the locus of the minimum acceleration points starts to deviate significantly from the trace of the primary orbit. When ρ drops to a critical value ρ^* which is sligtly larger than ρ_{L2} a plateau is encountered in which the value of the minimum control acceleration is almost constant for δ increasing up to its boundary limit $(\rho^* + 1)$ which is reached when the locus crosses the y axis. This means the locus describes a portion of a circumference centered at the second primary and along which the magnitude of the control aceeleration is virtually constant. As ρ further decreases the control acceleration, now directed away from the second primary, decreases until it becomes zero at $L2$. Reducing ρ even further will result in an increase in the magnitude of the control acceleration, now directed towards the second primary, until a jump occurs which brings the locus to the negative part of the x axis with ρ just slightly larger than ρ_{L1} and with negative radial acceleration. If ρ is further decreased we reach $L1$ with zero control acceleration. Finally, an increase in the required acceleration is encountered if one ones to obtain equilibrium at a distance smaller than ρ_{L1} in which case the spacecraft will be located on the negative x axis.

Now that the structure of the minimization problem has been clarified we can approach the problem analitically.

Once ρ is fixed, the value of δ that minimizes J obeys:

$$\frac{\partial J}{\partial \delta} = 0. \tag{26}$$

After performing the derivatives and with some algebraic simplifications Eq. (26) yields a 6-degree polynomial equation in $\delta(\rho)$:

$$\begin{aligned} &2\left(\rho^3-\mu\right)\delta^6 + \left(2\rho^3-\rho^3\mu-\mu\right)\delta^3 \\ &+3\mu\left(\rho^2-1\right)\left(\rho^3-1\right)\delta - 4\rho^3(1-\mu) = 0 \end{aligned} \tag{27}$$

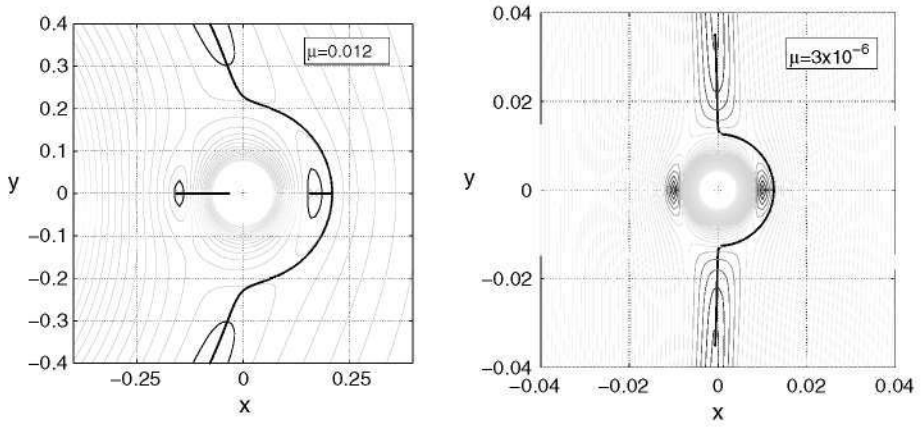

Fig. 4 Locus of the minimum control acceleration points (*dark line*) in the Earth–Moon system (*left*) and for the Sun–Earth system (*right*) for a given distance ρ from the second primary. A countour of the magnitude of the control acceleration is included (*grey lines*). The locus is computed numerically with a grid sampling approach

which can be numerically solved to obtain the optimum value δ_{opt}. It is important to point out that Eq. (27) only provides values of δ_{opt} corresponding to stationary points for $J(\rho, \delta)$. On the other hand, as we have just seen, when ρ is small enough the locus of the minimum control points is located on the x axis where $\rho = |\delta - 1|$ and the minima are not necessarily stationary points (see boundary condition 5) and cannot be derived through Eq. (27). Nevertheless Eq. (27) is effective in the derivation of all minimum acceleration points that do not belong to the x axis, and, in particular, the ones inside the stable equilibrium region previously identified. As μ is usually small, an approximate analytical solution can be found with a straightforward perturbation method (Nayfeh 1981). To this purpose we set:

$$\delta = \delta_0 + \mu\delta_1 + \mu^2\delta_2 + \mathcal{O}(\mu^3). \tag{28}$$

After substituting the latter into Eq. (27), expanding in a Taylor series for small μ, and solving each term we eventually find:

$$\delta_{opt} \cong \delta_0 + \mu\delta_1 + \mu^2\delta_2 = 1 + \frac{1-\rho^3}{6\rho}\mu - \frac{\rho^8 + 2\rho^6 - 2\rho^5 + 2\rho^3 + \rho^2 - 4}{36\rho^4}\mu^2 \tag{29}$$

which compared with the exact expression provided by Eq. (27) exhibits an error which increases exponentially with the inverse of the distance from the second primary. It can be seen later that all along the *stable equilibrium region* previously computed Eq. (29) provides an estimate of the optimal distance δ with a relative error on the second term:

$$e = \left| \frac{\delta_{opt} - 1 - \mu\delta_1}{\delta_{opt} - 1} \right|$$

which is less than 3%.

The corresponding control acceleration is readily computed by substituting Eq. (29) into Eqs. (8–25). Neglecting terms of order μ^2 and higher we obtain:

$$a = \sqrt{a_x^2 + a_y^2} \cong \frac{\mu}{\rho^2}\sqrt{1 - \frac{\rho^2 + 8\rho^3 - 2\rho^5 - 4\rho^6 + \rho^8}{4}} \tag{30}$$

Note that both Eqs. (29) and (30) are consistent with the location of the triangular Lagrangian points ($\rho = 1$) for which the control acceleration is zero.

The corresponding dimensional acceleration yields:

$$\hat{a} = \frac{GM_2}{\rho^2 \ell^2} \sqrt{1 - \frac{\rho^2 + 8\rho^3 - 2\rho^5 - 4\rho^6 + \rho^8}{4}} \tag{31}$$

Let us now look for an approximate analytical estimation of the minimum distance from the second primary allowing stability. This can be done by substituding the value of δ_{opt} (Eq. (29)) into conditions (16) and solving for ρ. After doing that and retaining terms up to μ^2(for the first condition) and μ (for the latter two) the three conditions read:

$$\begin{aligned} &47\rho^{10}\mu^2 + \left(-168\mu^2 + 60\mu\right)\rho^8 - 4\rho^7\mu^2 \\ &+ \left(12 - 120\mu + 108\mu^2\right)\rho^6 + \left(48\mu - 120\mu^2\right)\rho^5 \\ &-43\mu^2\rho^4 + \left(216\mu^2 - 312\mu\right)\rho^3 + 180\rho^2\mu^2 + 108\mu^2 > 0 \end{aligned} \tag{32}$$

$$-3\mu\rho^5 + 6\rho^3 + 3\mu\rho^2 - 6\mu > 0 \tag{33}$$

$$\begin{aligned} &-8\rho^{10}\mu - 4\left(3 - 7\mu\right)\rho^8 + \rho^7\mu + 8\left(3 - 2\mu\right)\rho^6 - \left(6 - 22\mu\right)\rho^5 \\ &+ 7\mu\rho^4 + 8\left(6 - 5\mu\right)\rho^3 - 32\rho^2\mu - 16\mu > 0 \end{aligned} \tag{34}$$

It can be verified that when $\mu < 0.1$, which encompasses the totality of Sun-planet and planet-satellite systems in our solar system, all terms of the type $\mu\rho^k$ in the above expression can be neglected with a maximum loss of accuracy not exceeding 5%. In this way the three contraints simplify to:

$$\rho^6 - 26\rho^3\mu + 9\mu^2 > 0, \tag{35}$$

$$\rho^3 - \mu > 0, \tag{36}$$

$$-2\rho^8 + 3\rho^6 - \rho^5 + 8\rho^3 - 16\mu > 0 \tag{37}$$

From the first two conditions we obtain our stability boundary limit:

$$\rho > \rho_{\min} = (13\mu + 4\mu\sqrt{10})^{1/3} \approx (26\mu)^{1/3} \tag{38}$$

It can be easily checked that condition (37) is always verified for $\rho > \rho_{\lim}$.

The corresponding control acceleration computed at the boundary of the stable region is:

$$a(\rho_{\min}) = \frac{(26\mu)^{1/3}\,|1 - 26\mu|\,\sqrt{4 - (26\mu)^{2/3}}}{52}$$

In dimensional units the minimum distance from the second primary in order to obtain open-loop stability with minimum control acceleration is finally:

$$r_{\min} \simeq \ell(26\mu)^{1/3} \tag{39}$$

And the required dimensional control acceleration (Eq. (30)) is:

$$\hat{a}(r_{\min}) \cong \frac{GM_2}{\mu\ell^2}\left[\frac{(26\mu)^{1/3}\,|1 - 26\mu|\,\sqrt{\left|4 - (26\mu)^{2/3}\right|}}{52}\right] \tag{40}$$

The intersections of the 2:1 and 3:1 resonance curves with the minimum control acceleration curve (Eq. (27)) can also be computed numerically. Nevertheless, similarily to what was done for the stability boundary, an approximate analytical expression that works very well

for $\mu < 0.1$ can be obtained by plugging Eq. (29) int Eqs. (23, 24) and neglecting all terms of the type $\mu\rho^k$. In this way we finally obtain the two intersections as:

$$\rho_{21} \simeq \left(\frac{79}{2}\mu\right)^{1/3} \quad ; \quad \rho_{31} \simeq \left(\frac{206}{3}\mu\right)^{1/3}$$

6 Applications

The fact that a spacecraft can be made to hover in the vicinity of a planet or satellite and kept stable with just a constant force is very appealing from a general point of view. On the other hand the interest and applicability of the concept in a real mission scenario depends on the chosen three-body gravitational system and has to take into account the following aspects:

1. The minimum stable hovering distance (Eq. (39)) should be as close as possible with the second primary in order to provide science and/or communication benefits
2. The minimum control acceleration (Eq. (40)) should be as small as possible so that it can be provided by state of the art solar sail and/or other low-thrust propulsion systems (Mengali and Quarta 2009; Curreli et al. 2010).

Table 1 lists the equilibrium characteristics of a number of selected candidate Sun-planet and planet-satellite systems. The four innermost planets enjoy favorable conditions in terms of minimum hovering distance, which is suitable for spacecraft communication purposes, and required acceleration, which could be easily supplied with state-of-the art solar sails (McInnes 2003b; Farres and Jorba 2010). Another important advantage is given by the fact that the sail orientation can be maintained with a fixed direction relative to the direction of both primaries and can be efficientlly repositioned at different azimuthal locations as proposed by McInnes (2003a).

Table 1 Selected candidate gravitational systems with minimum required distance and acceleration for stable hovering

	μ	ℓ (km)	$r_{\min}$ (km)	$a(r_{\min})$ (m/s^2)
Sun–Mercury	1.66×10^{-7}	5.8×10^{7}	9.4×10^{5}	2.5×10^{-5}
Sun–Venus	2.45×10^{-6}	1.08×10^{8}	4.3×10^{6}	1.7×10^{-5}
Sun–Earth	3.00×10^{-6}	1.50×10^{8}	6.4×10^{6}	9.7×10^{-6}
Sun–Mars	3.23×10^{-7}	2.28×10^{8}	4.6×10^{6}	2.0×10^{-6}
Earth–Moon	1.22×10^{-2}	3.89×10^{5}	2.6×10^{5}	4.5×10^{-5}
Mars–Phobos	1.67×10^{-8}	9.38×10^{3}	7.1×10^{1}	1.4×10^{-4}
Mars–Deimos	2.29×10^{-9}	2.35×10^{4}	9.2×10^{1}	1.2×10^{-5}
Saturn–Enceladus	1.90×10^{-7}	2.38×10^{5}	4.1×10^{3}	4.4×10^{-4}
Jupiter–Io	4.70×10^{-5}	4.22×10^{5}	4.5×10^{4}	2.9×10^{-3}
Jupiter–Europa	2.53×10^{-5}	6.71×10^{5}	5.8×10^{4}	9.4×10^{-4}
Jupiter–Metis	6.31×10^{-11}	1.28×10^{5}	1.5×10^{2}	3.5×10^{-4}
Jupiter–Adrastea	3.95×10^{-12}	1.29×10^{5}	6.0×10^{1}	1.4×10^{-4}
Jupiter–Amalthea	1.09×10^{-9}	1.81×10^{5}	5.5×10^{2}	4.5×10^{-4}
Jupiter–Thebe	7.89×10^{-10}	2.22×10^{5}	6.1×10^{2}	2.7×10^{-4}

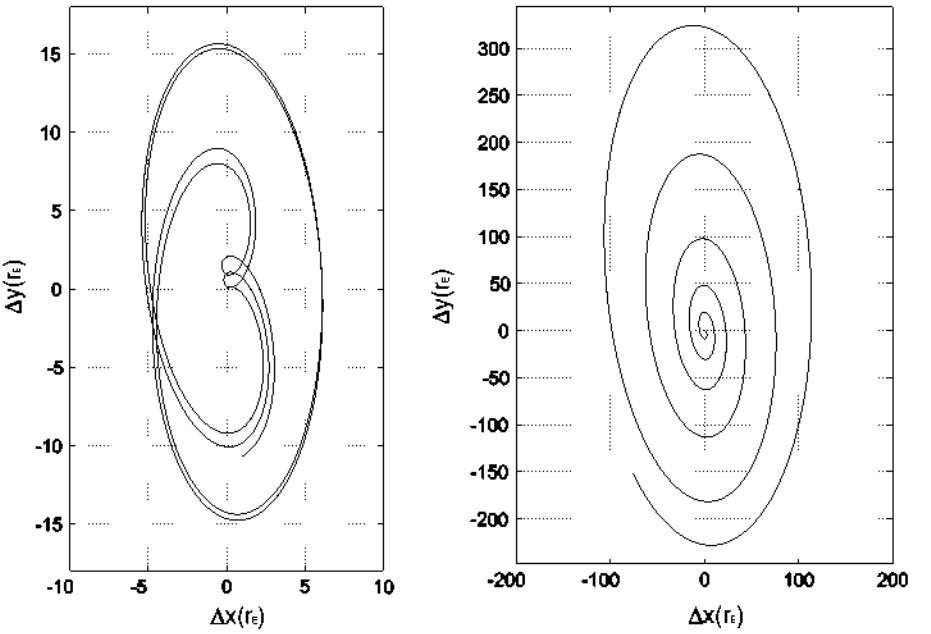

Fig. 5 Numerically-computed trajectories for a spacecraft located at a distance $\rho = (30\mu)^{1/3}$ (stable zone) and $\rho = (24.7\mu)^{1/3}$ (unstable) on the minimum-control curve for the Sun–Earth system ($\mu = 3.0 \times 10^{-6}$). A disturbance velocity is applied with 1 m/s magnitude and 45 degrees orientation with respect to the x axis in the positive xy plane (Fig. 1). The distance is measured in Earth radii (r_E) and the duration of the simulation is 50 years

For the different planet-satellite systems the case of Deimos seems to be the most favorable as an hovering spacecraft could be passively stabilized at about 100 km from the surface (i.e. less than 9 times the size of the satellite) with a relatively small acceleration. Finally we point out that the case of the inner Jupiter moons is also promising because the required control acceleration, probably too big for a solar sail, can be easily provided by electrodynamic tethers of modest size (see Pelaez and Scheeres 2007). Nevertheless the harsh radiation environment in the vicinity of Jupiter would make the last application prohibitive with current technology.

Before concluding the article we present numerical results supporting the analytical results obtained above. Figure 5 summarizes the stable/unstable behaviour of the 3-body dynamics for the case of the Earth–Sun system showing a stable behavior for $\rho > (26\mu)^{1/3}$.

7 Conclusions

We have investigated the properties of minimum-control artificial equilibrium points in the planar circular restricted three-body problem providing simple analytical expressions that characterize their location, required control acceleration and stability properties. It is seen that once the distance from the second primary is fixed and greater than the distance from the second collinear Lagrangian point minimum-control is obtained by having the spacecraft almost coorbiting with the second primary with an offset that is a simple function of the mass

ratio μ of the two primaries. The required control acceleration would then decrease until becoming zero as the spacecraft location approaches the nearest triangular libration point. Lyapunov stability under minimum control conditions is seen to occur as the distance with the second primary reaches the value $\rho_{\min} \simeq (26\mu)^{1/3}$ and taking the primaries' separation as unit of distance. As the spacecraft location moves away from the second primary along the minimum control curve, stability is always assured with the exclusion of 2:1 and 3:1 resonance conditions which appear at distances $\rho_{21} \simeq (79\mu/2)^{1/3}$ and $\rho_{31} \simeq (206\mu/3)^{1/3}$, respectively. A quick inspection of promising applications in our solar system shows that stable solar-sail-stabilized observatories or communication outposts coorbiting with Earth Venus and Mars are feasible from the point of view of the control acceleration required and advantageous given their vicinity with the planet of interest. Numerical simulations agree with the provided analytical formulas. Future work will be needed to assess the engineering feasibility of the concept.

Acknowledgments The authors would like to thank Prof. Ryan Russell (Georgia Tech) for his constructive comments and suggestions in the review process. The work was supported by the DGI of the Spanish Ministry of Education and Science (research grant ESP2007-64068).

References

Baig, S., McInnes, C.: Artificial three-body equilibria for hybrid low-thrust propulsion. J. Guid. Control Dyn. **31**(6), 1644–1655 (2008)

Celletti, A., Giorgilli, A.: On the stability of the lagrangian points in the spatial restricted problem of three-body. Celest. Mech. Dyn. Astron. **50**, 31–58 (1991)

Curreli, D., Lorenzini, E.C., Bombardelli, C., Sanjurjo-Rivo, M., Pelaez, J., Scheeres, D.: Three-body dynamics and self-powering of an electrodynamic tether in a plasmasphere. J. Propuls. Power **26**(3), 385–393 (2010)

Deprit, A., Deprit-Bartholome, A.: Stability of the triangular lagrangian points. Astron. J. **72**(2), 173–179 (1967)

Farres, A., Jorba, A.: Periodic and quasi-periodic motions of a solar sail close to SL 1 in the Earth–Sun system. Celest. Mech. Dyn. Astron. **107**, 233–253 (2010)

Forward, R.L.: Statite: A spacecraft that does not orbit. J. Spacecr. Rockets **28**(5), 606–611 (1991)

Leontovich, A.: On the stability of the lagrange periodic solutions of the restricted three-body problem. Dokl. Math. (in Russian) **3**, 425–428 (1962)

Markeev, A.: Stability of the triangular lagrangian solutions of the restricted three-body problem in the three-dimensional circular case. Sov. Astron. **15**(4), 682–686 (1972)

McInnes, C.: Azimuthal repositioning of payloads in heliocentric orbit Using solar sails. J. Guid. Control Dyn. **26**(4), 662–664 (2003)

McInnes, C.: Solar sailing: Mission applications and engineering challenges. Philos. Transact. R. Soc. London A Math. Phys. Eng. Sci. **361**(1813), 2989 (2003)

McInnes, C.R., McDonald, A.J.C., Simmons, J.F.L., MacDonald, E.W.: Solar sail parking in restricted three-body systems. J. Guid. Control Dyn. **17**(2), 399–406 (1994)

Mengali, G., Quarta, A.: Non-Keplerian orbits for electric sails. Celest. Mech. Dyn. Astron. **105**(1), 179–195 (2009)

Morimoto, M.Y., Yamakawa, H., Uesugi, K.: Artificial equilibrium points in the low-thrust restricted three-body problem. J. Guid. Control Dyn. **30**(5), 1563–1567 (2007)

Nayfeh, A.: Introduction to perturbation techniques. Wiley, New York (1981)

Pelaez, J., Scheeres, D.J.: A permanent tethered observatory at jupiter. Dynamical analysis. Adv. Astronaut. Sci. **127**(PART 2), 1307–1330 (2007)